HHS Public Access

Author manuscript

Magn Reson Imaging. Author manuscript; available in PMC 2018 February 01.

Published in final edited form as:

Magn Reson Imaging. 2017 February ; 36: 93–97. doi:10.1016/j.mri.2016.10.023.

Sex Differences in Sodium Deposition in Human Muscle and Skin

Ping Wang[a,b,*], **Muge Serpil Deger**[c], **Hakmook Kang**[d], **T. Alp Ikizler**[c], **Jens Titze**[e], and **John C. Gore**[a,b]

[a]Institute of Imaging Science, Vanderbilt University Medical Center, Nashville, TN, USA

[b]Department of Radiology and Radiological Sciences, Vanderbilt University Medical Center, Nashville, TN, USA

[c]Division of Nephrology and Hypertension, Department of Medicine, Vanderbilt University Medical Center, Nashville, TN, USA

[d]Department of Biostatistics, Vanderbilt University Medical Center, Nashville, TN, USA

[e]Division of Clinical Pharmacology, Department of Medicine, Vanderbilt University Medical Center, Nashville, TN, USA

Abstract

The aim of this work was to investigate possible sex differences in the patterns of sodium deposition between muscle and skin using sodium MRI. A total of 38 subjects were examined for comparisons: 20 males, aged 25–79 years with a median age of 51; 18 females, aged 38–66 years, median age 53. All subjects underwent sodium MRI scans of the calf muscles together with cross sections through four calibration standards containing known sodium contents (10mM, 20mM, 30mM, and 40mM). Tissue sodium concentrations (TSC) in muscle and skin were then calculated by comparing signal intensities between tissues and reference standards using a linear analysis. A Wilcoxon rank sum test was applied to the ΔTSC (= $TSC_{muscle} - TSC_{skin}$) series of males and females to examine if they were significantly different. Finally, a multiple linear regression was utilized to account for the effects from two potential confounders, age and body mass index (BMI). We found that sodium content appears to be higher in skin than in muscle for men, however women tend to have higher muscle sodium than skin sodium. This sex-relevant sodium deposition is statistically significant ($P = 3.10\times10^{-5}$) by the Wilcoxon rank sum test, and this difference in distribution seems to be more reliable with increasing age. In the multiple linear regression, gender still has a statistically significant effect ($P < 1.0\times10^{-4}$) on the difference between sodium deposition in muscle and skin, while taking the effects of age and BMI into account.

[*]**Address Correspondence:** Ping Wang, PhD., Vanderbilt University Institute of Imaging Science, B0104 MCN, 1161 21st Ave South, Vanderbilt University, Nashville, TN 37232-2310, p.wang@vanderbilt.edu, Tel: 615-936-3328, Fax: 615-936-7247.

Keywords

Sodium deposition; Muscle; Skin; Gender; Sodium MRI

1. Introduction

Sodium is the most abundant cation in the human body, and is vital for cellular function and integrity [1, 2]. Normally, the intracellular space accounts for 80% of tissue volume with a sodium concentration of 10 – 15mM, against an extracellular volume fraction of 20% with a sodium concentration of 140 – 150mM. This relatively stable concentration difference is primarily maintained by the sodium-potassium Na^+/K^+-ATPase pump, which pumps sodium out of cells while pumping potassium into cells. Leaky cell membranes or impaired Na^+/K^+ exchange kinetics potentially change the cytosolic total tissue sodium, making sodium a biomarker of a wide range of disease states [3–6], such as stroke, cancer, osteoarthritis, neurological disorders, edema, and acute myocardial infarction. Typically, an increase of total tissue sodium concentration (TSC) indicates a loss of tissue viability and is associated with an increase of intracellular sodium due to the loss of integrity of the cell, and also with an increase of extracellular volume when cells are dying [1, 7–12].

The first investigation of sodium NMR in biological tissues was piloted in the early 1970s [13, 14], while the feasibility of sodium MRI in human subjects and its potential use for detecting pathological changes were demonstrated in the middle to late 1980s [3, 8, 9, 15]. Interest in the use of sodium MRI has increased over time due to the availability of higher magnetic fields, improved hardware and pulse sequences [4, 16], and the availability of ultra-high field MRI scanners (7T and 9.4T) [17–19]. Further improvements in electronics, RF coils, and acquisition techniques [20–22] have made sodium MRI feasible at reasonable resolution in practical scan times. To date, sodium MRI has been applied to image several human organs *in vivo* including brain, heart, cartilage, kidney, breast, spine, as well as muscle and skin [6, 23–34].

In muscle, sodium changes can be linked to several disease states, including diabetes mellitus, starvation, hypothyroidism, hypertension, and cardiovascular risk. Skin sodium has been studied relatively rarely compared to muscle. Recent studies have shown that sodium may be sequestered in both skin and muscle so that tissue sodium levels are not reliably measured by sampling blood or interstitial fluid, which has important implications for the management of hypertension and kidney disease [33]. Therefore, measurements of sodium concentrations in skin or muscle may be a useful biomarker of risk of disease progressions, but the interpretation of such measurements will rely on understanding the factors that affect sodium levels.

A previous study observed that sodium in muscle and skin appeared to change differently with age for men and women. Specifically, it noted an increase of sodium storage in skin for both men and women, and an increase of sodium storage in muscle for men, but not women [33]. In our recent preliminary studies [35, 36], we observed that the sodium deposition between muscle and skin was sex-relevant. For males, skin sodium content appeared higher than muscle sodium, which was opposite to females who tended to have higher muscle

sodium than skin. Prompted by these observations, we investigate whether this sex specific pattern of sodium deposition in muscle and skin is statistically significant.

2. Materials and methods

This study was approved by the Institutional Review Board (IRB) of the Vanderbilt University. A total of thirty eight (38) subjects: 20 males, aged 25–79 with a median age of 51; 18 females, aged 38–66 years, with a median age of 53 were recruited. The demographic characteristics of the subjects are included in Table 1. Written informed consent from each subject was obtained prior to MR imaging.

2.1. MR acquisition

Imaging was performed on a Philips Achieva 3.0T MR scanner (Philips Healthcare, Cleveland OH, USA) with a ^{23}Na quadrature knee coil (Rapid Biomedical GmbH, Rimpar, Germany). Four calibration phantoms (NaCl aqueous solutions of 10mM, 20mM, 30mM, and 40mM) served as reference standards and were scanned together with sections through the subject's calf muscles. Each subject was required to rest for 30 minutes before imaging to allow the body to reach a physiological equilibrium. The left lower leg (the widest part of calf region) was scanned with the skin closely in contact with the hard surface of the phantom holder. Fig. 1 shows the sodium coil, phantoms and holder, and the subject's setup.

MR scans primarily included a proton mDixon scan and a sodium scan. The mDixon scan provides a high resolution anatomical image allowing for accurate muscle ROI (region of interest) definition. Five 6mm slices were acquired by the scanner body coil with parameters FOV = 192 × 192 mm^2, resolution = 1 × 1 mm^2, TR = 200ms, and TE = 4.6 ms. Four types of images (water, water fat in-phase, water fat out-of-phase, and fat) were generated resulting in a total of 20 images. Scan time was 3 min 52 sec. For sodium relaxation, muscle typically has a T_1 of 12 – 25ms, a short T_2 ($T_{2,\,short}$) of 1.5 – 2.5ms, and a long T_2 ($T_{2,\,long}$) of 15 – 30ms [2]. To our knowledge, skin relaxation times are not readily available, so we assume that they are within a similar range as muscle. To eliminate the T_1 effect in tissues, a TR of approximately $5T_{1,\,tissue}$ was chosen to allow the longitudinal magnetization to fully relax, and the shortest possible TE was chosen to maximize SNR (signal-to-noise ratio). Aqueous NaCl solution has a T_2 (long component only) that is close to its T_1 ranging from 50 – 60ms [5, 37]. Although longitudinal magnetization in the phantom is not fully relaxed for the selected TR, higher SNR would be achieved by increasing the number of signal averages for a given total scan time. In view of these factors, sodium imaging was performed using an optimized 3D Gradient-echo sequence, with parameters FOV = 192 × 192 × 210mm^3, voxel size = 3 × 3 × 30mm^3, 7 slices, TR/TE/FA = 130ms/0.99ms/90°, bandwidth = 434Hz/pixel, acquisitions: 26, scan time = 15 min 54 sec. Prior to human imaging, the sodium coil homogeneity was examined on a plastic jar phantom (inner diameter = 14 cm, volume = 3.5L) filled with a 50mM aqueous NaCl solution using the above sodium imaging technique. A uniform sodium image was acquired (Fig. 2) indicating the imaging data acquired by the coil can be used reliably for sodium quantification without further B_1 calibration. All the human imaging data were processed off-line with custom MATLAB (R2013a) scripts.

2.2. Data processing

The mDixon and sodium scans were aligned in the middle of their imaging slabs, so that the center slice of each modality was taken for ROI definition and sodium quantification. The muscle ROIs included five regions (anterior compartment, peroneus, soleus, medial gastrocnemius, and lateral gastrocnemius) which were drawn on the mDixon images. Skin ROI and phantom ROIs were drawn on the sodium image directly, see Fig. 3.

Sodium quantification was performed by comparing signal intensities between tissue and calibration phantoms on the sodium image. A linear relationship (sodium concentration *vs* signal intensity) was assessed based on the phantom data, and results from a linear regression were applied to the tissue regions to quantify sodium content assuming the same T_1 and T_2 values for tissue and solutions. ImageJ (NIH, version 1.49v) was used for drawing ROIs and making signal intensity measurements.

2.3. Statistical analysis

Sodium differences between muscle and skin were computed for each subject ($\Delta TSC = TSC_{muscle} - TSC_{skin}$), and a Wilcoxon rank sum test was applied to the ΔTSC series of males and females to examine if they were significantly different (with P value reported).

To further examine contributions from other factors, a multiple linear regression model was applied in which sodium difference was the outcome variable and gender was the main explanatory variable while two potential confounders, i.e., age and BMI (body mass index) were added to the model.

In addition, a scatter plot was used to depict the relationship between ΔTSC and age for all subjects, and the correlation was examined by a linear regression analysis.

3. Results

Table 1 summarizes the demographic information and TSC in muscle and skin for males and females, along with the calculation of ΔTSC ($= TSC_{muscle} - TSC_{skin}$). Notably, a majority of the males have higher TSC in skin than in muscle, while female muscle TSC is greater than skin TSC. The Wilcoxon rank sum test confirms the sex difference in sodium deposition between muscle and skin is significantly different ($P = 3.10\times10^{-5}$). The multiple linear regression also showed a statistically significant effect of sex ($P < 1.0\times10^{-4}$) on the difference between sodium deposition in muscle and skin, while taking the effects of age and BMI into account.

Fig. 4 plots the correlation between sodium difference ($\Delta TSC = TSC_{muscle} - TSC_{skin}$) and age for males and females. Younger subjects appear to have lower |ΔTSC|, but it is more variable in males. The absolute value of ΔTSC tends to increase with increased age for both males and females, which is verified by the linear regressions (females: r = 0.41, $P = 0.089$; males: r = 0.57, $P = 0.0084$. Here r represents correlation coefficient).

4. Discussion

Our results show there are different patterns of sodium accumulation in muscle and skin for men and women, a difference that appears to increase with age. The MRI method used is able to unambiguously differentiate sodium in muscles and skin of the leg and quantify spatial differences in concentration with good precision and spatial resolution. These findings are relevant to the interpretation of sodium measurements that may be used to follow changes over time in, for example, patients with hypertension or chronic kidney disease.

Skin is an important site for extrarenal regulation of sodium metabolism. There is evidence that the skin interstitium concentrates electrolytes and thereby may provide a physiological barrier which induces a continuous solvent drag for water, very similar to the renal medullary interstitium. However, the physiological function of this process is not well characterized. It has also been suggested that sodium storage in skin may be relevant in health and disease [32, 33], but the mechanisms of sodium ions entry into the skin, and its clearance from interstitial tissue, still remain unclear [38].

In this study, we found gender differences of sodium deposition between muscle and skin. Men show higher sodium content in skin than in muscle, which is contrary to women who tend to accumulate higher muscle than skin sodium. Whether such differences reflect differences in sodium metabolic patterns or possibly the influence of other factors such as skin thickness and lipid content, which may be different amongst the sexes, remains unclear.

There are certain aspects can be further improved in our study. First, although it is reasonable for sodium imaging, the in-plane resolution of our sodium image (3mm × 3mm) is relatively low, which could be improved at higher field (such as 7T) and/or with more advanced UTE-like sequences. Second, the measured sodium signal was from both intracellular and extracellular spaces in our study. To be more specific for the underlying pathologic process, a selective assessment of the intra- or extracellular sodium might be more indicative. Prospective MRI approaches for selecting intra- or extracellular sodium could be based on inversion recovery (IR) [39, 40] or multiple quantum filter (such as double quantum filter - DQF, triple quantum filter - TQF), although the latter would need more investigation due to the large specific absorption rate (SAR) [41–43]. Moreover, $T_{2,\,short}$ and $T_{2,\,long}$ components in biological tissues constitute roughly 60% and 40% of the transverse magnetization [44]. There is often considerable signal loss in tissues due to the rapid decay of $T_{2,\,short}$ components when TE is not sufficiently short. Therefore, although such effects do not influence the conclusions of this study, sodium levels reported may not be accurate in an absolute sense because they assume equal relaxation times for sodium in tissue and the phantoms, which may underestimate the levels of sodium in tissue.

In conclusion, a significant sex dependent difference in sodium deposition between muscle and skin was found, with males having higher sodium content in skin than in muscle, while females have higher muscle sodium than skin sodium. This observation appears to be more reliable with increased age.

Acknowledgments

The work was supported by NIH T32 EB001628, and the Vanderbilt University Institute of Imaging Science (VUIIS) internal funds.

References

1. Madelin G, Lee JS, Regatte RR, Jerschow A. Sodium MRI: methods and applications. Prog Nucl Magn Reson Spectrosc. 2014; 79:14–47. [PubMed: 24815363]
2. Madelin G, Regatte RR. Biomedical applications of sodium MRI in vivo. J Magn Reson Imaging. 2013; 38(3):511–29. [PubMed: 23722972]
3. Ouwerkerk R. Sodium magnetic resonance imaging: from research to clinical use. J Am Coll Radiol. 2007; 4(10):739–41. [PubMed: 17903762]
4. Boada FE, Gillen JS, Shen GX, Chang SY, Thulborn KR. Fast three dimensional sodium imaging. Magn Reson Med. 1997; 37(5):706–15. [PubMed: 9126944]
5. Constantinides CD, Gillen JS, Boada FE, Pomper MG, Bottomley PA. Human skeletal muscle: sodium MR imaging and quantification-potential applications in exercise and disease. Radiology. 2000; 216(2):559–68. [PubMed: 10924586]
6. Inglese M, Madelin G, Oesingmann N, Babb JS, Wu W, Stoeckel B, Herbert J, Johnson G. Brain tissue sodium concentration in multiple sclerosis: a sodium imaging study at 3 tesla. Brain. 2010; 133(Pt 3):847–57. [PubMed: 20110245]
7. Ouwerkerk R. Sodium MRI. Methods Mol Biol. 2011; 711:175–201. [PubMed: 21279602]
8. Grodd W, Klose U. Sodium-MR-imaging of the brain: initial clinical results. Neuroradiology. 1988; 30(5):399–407. [PubMed: 2850509]
9. Hilal SK, Maudsley AA, Ra JB, Simon HE, Roschmann P, Wittekoek S, Cho ZH, Mun SK. In vivo NMR imaging of sodium-23 in the human head. J Comput Assist Tomogr. 1985; 9(1):1–7. [PubMed: 3968256]
10. Boada FE, LaVerde G, Jungreis C, Nemoto E, Tanase C, Hancu I. Loss of cell ion homeostasis and cell viability in the brain: what sodium MRI can tell us. Curr Top Dev Biol. 2005; 70:77–101. [PubMed: 16338338]
11. Hashimoto T, Ikehira H, Fukuda H, Yamaura A, Watanabe O, Tateno Y, Tanaka R, Simon HE. In vivo sodium-23 MRI in brain tumors: evaluation of preliminary clinical experience. Am J Physiol Imaging. 1991; 6(2):74–80. [PubMed: 1867865]
12. Winkler SS. Sodium-23 magnetic resonance brain imaging. Neuroradiology. 1990; 32(5):416–20. [PubMed: 2259436]
13. Berendsen HJ, Edzes HT. The observation and general interpretation of sodium magnetic resonance in biological material. Ann NY Acad Sci. 1973; 204:459–85. [PubMed: 4513164]
14. Magnuson JA, Magnuson NS. NMR studies of sodium and potassium in various biological tissues. Ann NY Acad Sci. 1973; 204:297–309. [PubMed: 4513156]
15. Ra JB, Hilal SK, Oh CH, Mun IK. In vivo magnetic resonance imaging of sodium in the human body. Magn Reson Med. 1988; 7(1):11–22. [PubMed: 3386516]
16. Boada FE, Christensen JD, Gillen JS, Thulborn KR. Three-dimensional projection imaging with half the number of projections. Magn Reson Med. 1997; 37(3):470–7. [PubMed: 9055238]
17. Atkinson IC, Lu A, Thulborn KR. Characterization and correction of system delays and eddy currents for MR imaging with ultrashort echo-time and time-varying gradients. Magn Reson Med. 2009; 62(2):532–7. [PubMed: 19353662]
18. Atkinson IC, Lu A, Thulborn KR. Preserving the accuracy and resolution of the sodium bioscale from quantitative sodium MRI during intrasubject alignment across longitudinal studies. Magn Reson Med. 2012; 68(3):751–61. [PubMed: 22139900]
19. Wang L, Wu Y, Chang G, Oesingmann N, Schweitzer ME, Jerschow A, Regatte RR. Rapid isotropic 3D-sodium MRI of the knee joint in vivo at 7T. J Magn Reson Imaging. 2009; 30(3): 606–14. [PubMed: 19711406]

20. Nagel AM, Laun FB, Weber MA, Matthies C, Semmler W, Schad LR. Sodium MRI using a density-adapted 3D radial acquisition technique. Magn Reson Med. 2009; 62(6):1565–73. [PubMed: 19859915]
21. Gurney PT, Hargreaves BA, Nishimura DG. Design and analysis of a practical 3D cones trajectory. Magn Reson Med. 2006; 55(3):575–82. [PubMed: 16450366]
22. Lu A, Atkinson IC, Claiborne TC, Damen FC, Thulborn KR. Quantitative sodium imaging with a flexible twisted projection pulse sequence. Magn Reson Med. 2010; 63(6):1583–93. [PubMed: 20512862]
23. Malzacher M, Kalayciyan R, Konstandin S, Haneder S, Schad LR. Sodium-23 MRI of whole spine at 3 Tesla using a 5-channel receive-only phased-array and a whole-body transmit resonator. Z Med Phys. 2015
24. Ouwerkerk R, Jacobs MA, Macura KJ, Wolff AC, Stearns V, Mezban SD, Khouri NF, Bluemke DA, Bottomley PA. Elevated tissue sodium concentration in malignant breast lesions detected with non-invasive 23Na MRI. Breast Cancer Res Treat. 2007; 106(2):151–60. [PubMed: 17260093]
25. Zollner FG, Konstandin S, Lommen J, Budjan J, Schoenberg SO, Schad LR, Haneder S. Quantitative sodium MRI of kidney. NMR Biomed. 2015
26. Newbould RD, Miller SR, Upadhyay N, Rao AW, Swann P, Gold GE, Strachan RK, Matthews PM, Taylor PC, Brown AP. T1-weighted sodium MRI of the articulator cartilage in osteoarthritis: a cross sectional and longitudinal study. PLoS One. 2013; 8(8):e73067. [PubMed: 23940822]
27. Staroswiecki E, Bangerter NK, Gurney PT, Grafendorfer T, Gold GE, Hargreaves BA. In vivo sodium imaging of human patellar cartilage with a 3D cones sequence at 3 T and 7 T. J Magn Reson Imaging. 2010; 32(2):446–51. [PubMed: 20677276]
28. Graessl A, Ruehle A, Waiczies H, Resetar A, Hoffmann SH, Rieger J, Wetterling F, Winter L, Nagel AM, Niendorf T. Sodium MRI of the human heart at 7.0 T: preliminary results. NMR Biomed. 2015
29. Resetar A, Hoffmann SH, Graessel A, Winter L, Waiczies H, Ladd ME, Niendorf T, Nagel AM. Retrospectively-Gated CINE Na Imaging of the Heart at 7.0Tesla Using Density-Adapted 3D Projection Reconstruction. Magn Reson Imaging. 2015
30. Nielles-Vallespin S, Weber MA, Bock M, Bongers A, Speier P, Combs SE, Wohrle J, Lehmann-Horn F, Essig M, Schad LR. 3D radial projection technique with ultrashort echo times for sodium MRI: clinical applications in human brain and skeletal muscle. Magn Reson Med. 2007; 57(1):74–81. [PubMed: 17191248]
31. Qian Y, Zhao T, Zheng H, Weimer J, Boada FE. High-resolution sodium imaging of human brain at 7 T. Magn Reson Med. 2012; 68(1):227–33. [PubMed: 22144258]
32. Kopp C, Linz P, Wachsmuth L, Dahlmann A, Horbach T, Schofl C, Renz W, Santoro D, Niendorf T, Muller DN, Neininger M, Cavallaro A, Eckardt KU, Schmieder RE, Luft FC, Uder M, Titze J. (23)Na magnetic resonance imaging of tissue sodium. Hypertension. 2012; 59(1):167–72. [PubMed: 22146510]
33. Kopp C, Linz P, Dahlmann A, Hammon M, Jantsch J, Muller DN, Schmieder RE, Cavallaro A, Eckardt KU, Uder M, Luft FC, Titze J. 23Na magnetic resonance imaging-determined tissue sodium in healthy subjects and hypertensive patients. Hypertension. 2013; 61(3):635–40. [PubMed: 23339169]
34. Nagel AM, Amarteifio E, Lehmann-Horn F, Jurkat-Rott K, Semmler W, Schad LR, Weber MA. 3 Tesla sodium inversion recovery magnetic resonance imaging allows for improved visualization of intracellular sodium content changes in muscular channelopathies. Invest Radiol. 2011; 46(12): 759–66. [PubMed: 21750464]
35. Wang, P.; Nockowski, C.; Gore, J. In vivo sodium T1 and T2 measurements in human calf at 3T. Proceedings of the 23rd Annual Meeting of ISMRM; Toronto, Ontario, Canada. 2015. p. 705
36. Wang, P.; Esteve, I.; Nockowski, C.; Gore, J. Correction for T1 effects on MRI estimation of muscle sodium levels. Proceedings of the 23rd Annual Meeting of ISMRM; Toronto, Ontario, Canada. 2015. p. 3237
37. Chang DC, Woessner DE. Spin-Echo Study of 23Na Relaxation in Skeletal Muscle. Evidence of Sodium Ion Binding inside a Biological Cell. J Magn Reson. 1978; 30(2):185–91.

38. Hofmeister LH, Perisic S, Titze J. Tissue sodium storage: evidence for kidney-like extrarenal countercurrent systems? Pflugers Arch. 2015; 467(3):551–8. [PubMed: 25600900]

39. Stobbe R, Beaulieu C. In vivo sodium magnetic resonance imaging of the human brain using soft inversion recovery fluid attenuation. Magn Reson Med. 2005; 54(5):1305–10. [PubMed: 16217782]

40. Madelin G, Lee JS, Inati S, Jerschow A, Regatte RR. Sodium inversion recovery MRI of the knee joint in vivo at 7T. J Magn Reson. 2010; 207(1):42–52. [PubMed: 20813569]

41. Eliav U, Navon G. Analysis of double-quantum-filtered NMR spectra of 23Na in biological tissues. J Magn Reson B. 1994; 103(1):19–29. [PubMed: 8137068]

42. Zhang Y, Poirer-Quinot M, Springer CS Jr, Balschi JA. Discrimination of intra- and extracellular 23Na+ signals in yeast cell suspensions using longitudinal magnetic resonance relaxography. J Magn Reson. 2010; 205(1):28–37. [PubMed: 20430659]

43. Knubovets T, Shinar H, Navon G. Quantification of the contribution of extracellular sodium to 23Na multiple-quantum-filtered NMR spectra of suspensions of human red blood cells. J Magn Reson. 1998; 131(1):92–6. [PubMed: 9533910]

44. Ouwerkerk R, Weiss RG, Bottomley PA. Measuring human cardiac tissue sodium concentrations using surface coils, adiabatic excitation, and twisted projection imaging with minimal T2 losses. J Magn Reson Imaging. 2005; 21(5):546–55. [PubMed: 15834912]

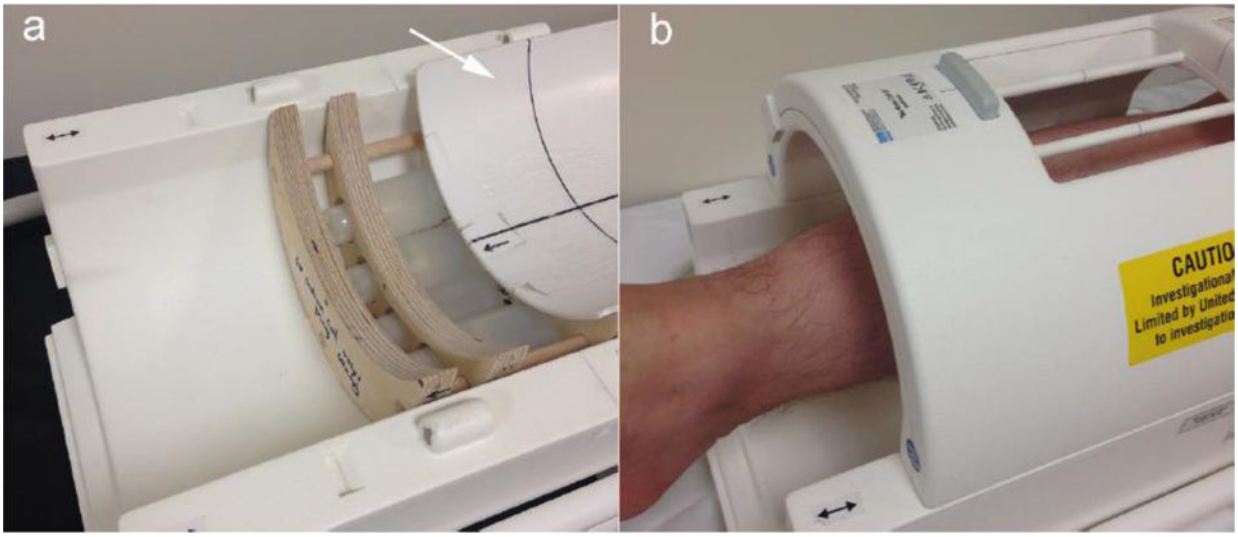

Fig. 1.

(a) Lower part of the 3T sodium knee coil. Inside the coil there are four calibration standards fixed in a phantom holder. A concave cover with a hard smooth surface (as pointed out by the white arrow) is slid open to display the phantoms. (b) During imaging, the skin is in direct contact with the surface of the cover.

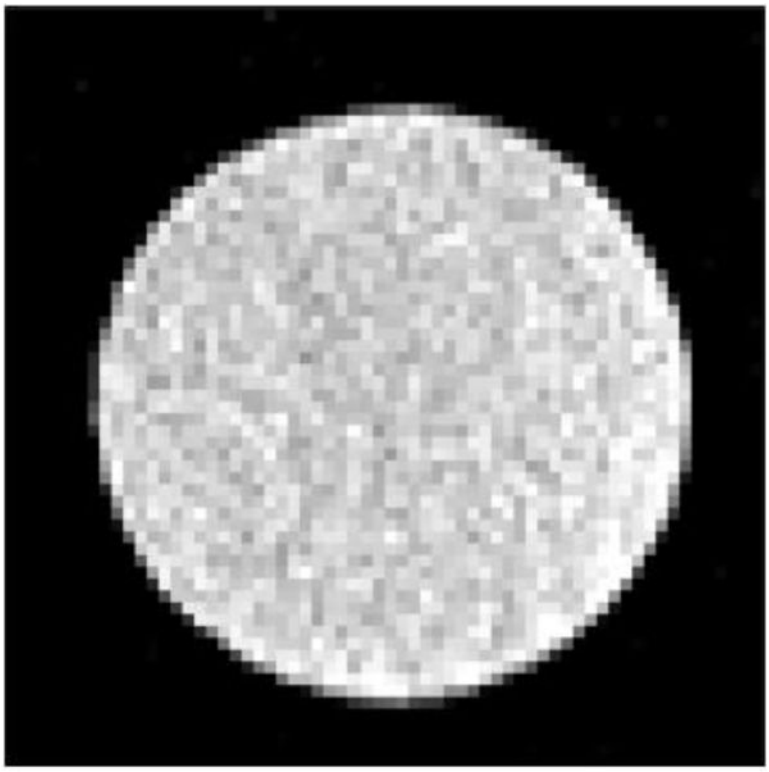

Fig. 2.

Sodium image on a plastic jar phantom (inner diameter = 14cm, volume = 3.5L) filled with a 50mM aqueous NaCl solution to evaluate the sodium coil homogeneity. The phantom image was acquired using the same sodium imaging technique as for human imaging. Since the image was highly uniform, B_1 calibration was unnecessary.

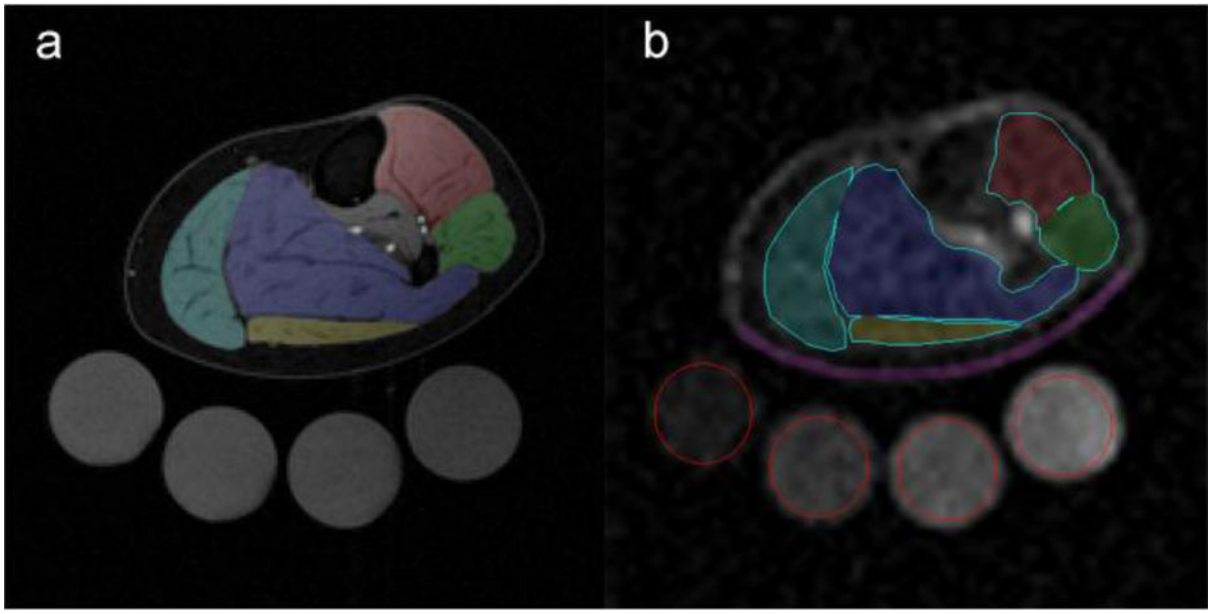

Fig. 3.

(a) mDixon water image of the lower leg with five muscle subgroups labeled: anterior compartment (including tibialis anterior and extensor digitorum longus) - red, peroneus - green, soleus - blue, medial gastrocnemius - cyan, and lateral gastrocnemius - gold. (b) The sodium image was interpolated to the same in-plane resolution as the mDixon image to directly overlay the muscle regions defined on (a). These regions were adjusted to exclude vessel pixels as well as to reduce partial volume effects. The skin ROI (purple) was drawn on the sodium image along the cross section of the concave cover, and phantom ROIs were drawn on sodium image as indicated by the red circles (left to right corresponds to sodium concentrations of 10mM, 20mM, 30mM, and 40mM).

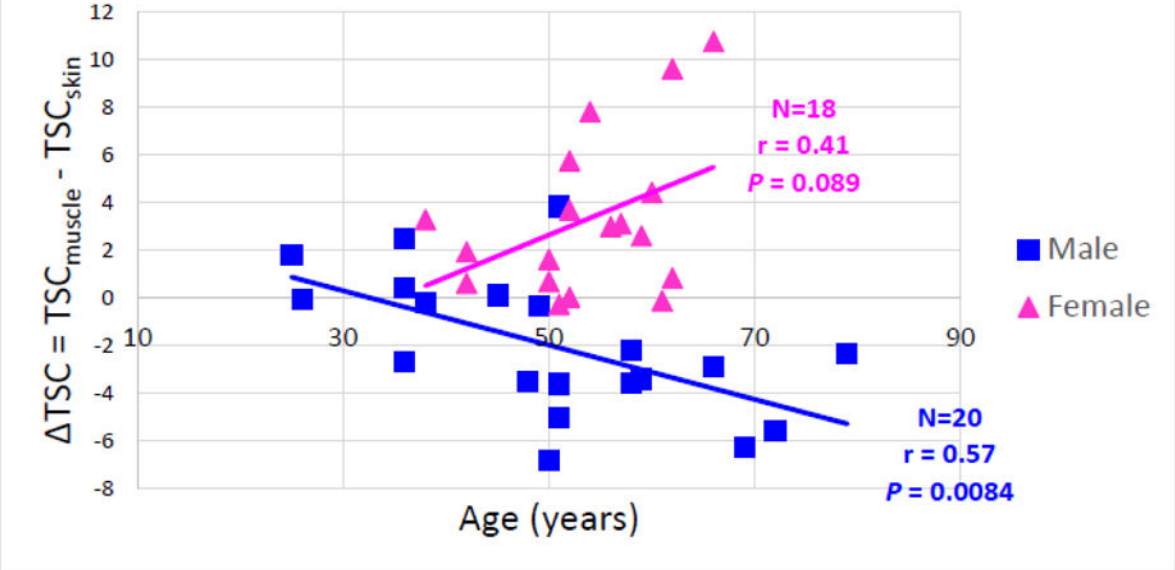

Fig. 4.

Scatter plot of ΔTSC = (TSC_{muscle} − TSC_{skin}) *versus* age for male group (blue) and female group (pink). |ΔTSC| appears to increase with the increase of age for both males and females, which is supported by the linear regressions (with correlation coefficient r and *P* value reported). Note that the ΔTSC of males tends to be more variable in younger subjects.

Table 1

Summary of demographic characteristics and sodium concentration in muscle and skin for male and female groups. Sodium difference (ΔTSC) between muscle and skin was computed as the input for a Wilcoxon rank sum test to examine the sex relevance of sodium distribution (in muscle and skin). A significant difference is observed ($P = 3.10\times10^{-5}$), with males having greater sodium in skin than in muscle, while females have higher muscle sodium than skin sodium. When using a multiple linear regression to account for the effects of age and BMI, sex is still the statistically significant determinant ($P < 1.0\times10^{-4}$) of the difference between sodium deposition in muscle and skin.

Age (years)	Sex [a]	Height (metre)	Weight (kg)	Body Mass Index (BMI)	Race [b]	TSC (mM)			Wilcoxon rank sum test
						Muscle	Skin	ΔTSC (muscle-skin)	
72	M	1.83	85.0	25.4	W	18.75	24.36	−5.61	
58	M	1.78	71.2	22.5	W	13.23	16.85	−3.62	
79	M	1.72	72.3	24.4	W	15.67	18.02	−2.34	
66	M	1.89	98.9	27.7	W	17.98	20.87	−2.89	
51	M	1.83	93.0	27.8	W	14.96	18.59	−3.62	
45	M	1.91	111.0	30.4	AA	17.36	17.26	0.10	
49	M	1.81	102.9	31.4	W	17.70	18.04	−0.34	
51	M	1.87	88.6	25.3	AA	18.43	14.60	3.83	
69	M	1.73	105.0	35.1	W	16.85	23.15	−6.30	
48	M	1.75	82.7	27.0	AA	15.66	19.18	−3.52	
36	M	1.72	96.0	32.4	AA	18.30	15.82	2.48	
25	M	1.80	75.7	23.4	AA	19.53	17.73	1.79	$P \approx 3.10 \times 10^{-5}$
36	M	1.79	129.2	40.3	AA	14.18	13.75	0.43	
50	M	1.86	97.9	28.3	AA	19.08	25.94	−6.85	
58	M	1.80	91.4	28.2	W	18.53	20.75	−2.21	
59	M	1.83	79.4	23.7	W	14.69	18.12	−3.42	
51	M	1.85	136.5	39.9	AA	18.48	23.50	−5.02	
38	M	1.75	81.6	26.6	W	17.20	17.44	−0.23	
36	M	1.78	72.6	22.9	W	15.15	17.85	−2.70	
26	M	1.70	77.1	26.7	A	14.91	14.98	−0.067	
61	F	1.65	88.9	32.7	W	15.46	15.59	−0.13	
56	F	1.51	53.5	23.5	W	17.10	14.11	2.99	
54	F	1.70	47.4	16.4	W	24.76	16.94	7.81	

Age (years)	Sex [a]	Height (metre)	Weight (kg)	Body Mass Index (BMI)	Race [b]	TSC (mM)			Wilcoxon rank sum test
						Muscle	Skin	ΔTSC (muscle-skin)	
59	F	1.62	83.8	31.9	W	15.00	12.40	2.60	
62	F	1.63	62.0	23.3	AA	22.44	12.81	9.62	
60	F	1.69	65.1	22.8	W	15.19	10.76	4.42	
50	F	1.68	63.1	22.4	W	14.54	13.86	0.67	
52	F	1.66	102.5	37.2	AA	16.98	13.31	3.67	
52	F	1.66	79.3	28.8	W	17.34	17.32	0.01	
57	F	1.62	53.5	20.4	W	14.56	11.45	3.10	
51	F	1.60	54.4	21.3	W	17.33	17.62	−0.28	
50	F	1.74	66.8	22.1	W	15.96	14.35	1.61	
42	F	1.52	81.0	35.1	AA	14.23	13.62	0.61	
66	F	1.59	70.0	27.7	AA	25.74	14.97	10.77	
52	F	1.68	83.7	29.7	AA	26.76	21.01	5.75	
62	F	1.68	78.2	27.7	W	21.31	20.48	0.82	
42	F	1.62	90.6	34.5	AA	15.30	13.38	1.92	
38	F	1.58	68.0	27.2	A	13.83	10.54	3.28	

[a] Abbreviations of sex: M – Male, F – Female.

[b] Abbreviations of race: W – While, AA – African American, A – Asian.